

This is the pre-peer reviewed version of the following article: Poosapati, Aswani, Karla Negrete, Micah Thorpe, John Hutchison, Mark Zupan, Yucheng Lan, and Deepa Madan. "Safe and Flexible Chitosan-Based Polymer Gel as an Electrolyte for Use in Zinc-Alkaline Based Chemistries." Journal of Applied Polymer Science 138, no. 33 (2021): 50813. <https://doi.org/10.1002/app.50813>., which has been published in final form at <https://doi.org/10.1002/app.50813>. This article may be used for non-commercial purposes in accordance with Wiley Terms and Conditions for Use of Self-Archived Versions.

Access to this work was provided by the University of Maryland, Baltimore County (UMBC) ScholarWorks@UMBC digital repository on the Maryland Shared Open Access (MD-SOAR) platform.

Please provide feedback

Please support the ScholarWorks@UMBC repository by emailing scholarworks-group@umbc.edu and telling us what having access to this work means to you and why it's important to you. Thank you.

Safe and flexible chitosan-based polymer gel as an electrolyte for use in Zinc-alkaline based chemistries

Aswani Poosapati¹, Karla Negrete¹, Micah Thorpe¹, John Hutchison¹, Marc Zupan¹, Yucheng Lan² and Deepa Madan^{1,*}

¹ Department of Mechanical Engineering, University of Maryland, Baltimore County, MD 21250, USA.

² Department of Physics, Morgan state university, Baltimore, MD 21251, USA.

* Address all **correspondence** to Dr. Deepa Madan at **deemadan@umbc.edu**

ABSTRACT

A novel flexible, high performing chitosan-based gel electrolyte with poly (vinyl alcohol) (PVA) and potassium hydroxide (KOH) additives is prepared, using an optimized energy and time efficient method. Incorporation of a gel-based electrolyte in batteries aims to eliminate safety hazards present within conventional liquid-based electrolyte constructions. The ionic conductivity values obtained at room temperature are in the range of 5.32 - 105 mS/cm depending on composition. Optical, Scanning-electron microscopy, X-ray diffraction (XRD) and Fourier transform infrared (FT-IR) spectra studies are conducted to understand morphological and structural changes in the films with additives. Thermogravimetric analysis (TGA), manual bending and tensile tests, linear scan and cyclic voltammetry (LSV, CV) analysis are also conducted to study the physical and electrochemical stability of the films. Also, the prepared electrolytes are incorporated to form Zn-MnO₂ batteries and tested. Results reveal no physical damage of the films under continuous bending over 250 cycles. Mechanical properties for CPK0.3 suggest a strong and ductile material well suited for the intended application. Additionally, the novel electrolyte exhibits excellent physical stability up to 50°C, electrochemical stability until 2V for Zinc

electrodes and prove to successfully accommodate redox reactions involved in the Zn-MnO₂ alkaline system.

Keywords

Polymer electrolyte, flexible, chitosan, poly (vinyl alcohol), potassium hydroxide.

1. INTRODUCTION

The need for reliable, scalable, and efficient energy storage mechanisms has propelled much of the secondary battery research present in current day ^{1,2}. It is well established that in any kind of rechargeable batteries, an electrolyte plays a major role in the performance of the complete cell since it is the interface at which all the redox reactions responsible for releasing or storing energy in a battery occur in addition to the electrodes themselves ^{3,4}. Hence its development is crucial towards advancements of an electrochemical system. Throughout the development from liquid to solid based systems, polymer-based electrolytes have attracted a lot of attention for research due to their added advantages such as non-toxicity, lack of leakage issues, eliminating the need for separators, suppressing dendrite propagation through mechanical force, lightweight, and also boosting its application in flexible energy storage systems ³⁻²⁴. A vast variety of polymers such as polyacrylonitrile (PAN), polyethylene oxide (PEO), polyvinyl alcohol (PVA), polymethylmethacrylate (PMMA), poly (vinylidene fluoride) (PVDF), poly(vinylpyrrolidone) (PVP), polyethylene glycol (PEG), poly(vinyl chloride) (PVC), polyacrylamide (PAM), cellulose from wood etc. have been explored with varying additives for different chemistries ⁵⁻²⁴. The reported performances were comparable to the liquid electrolytes.

Wu et al. demonstrated that radical polymerization can be used within a PVA-KOH system with

the addition of poly (acrylic acid) (PAA) to achieve a very high ionic conductivity (σ_i) of 0.301S/cm, but encountered a reduction in power density of zinc-air cells¹². Following which Merle et al. further crosslinked PVA-KOH with poly (ethylene glycol) diglycidyl ether (PEGDE) to improve the ionic conductivity of the electrolyte but found σ_i to slightly reduce to 0.22S/cm¹⁸. Santos et al. formed hydrogels using the same PVA-KOH system and reported a fairly similar value of σ_i (0.34S/cm)¹⁹ as Wu et al. Decent ionic conductivities for polymer electrolytes were already reported, however most of the gel preparation processes involved complex stages for synthesis and were time and energy intensive⁵⁻²⁰. There were also reported instances of gel electrolytes of the aforementioned compositions facing issues such as the over-insulation of the polymer itself especially at lower temperatures. Likely this is due to blockages present in many of the polymer's crystalline nature, limited flexibility of the gel-electrolyte, high interfacial resistance due to poor solubility of salts, and poor adhesion between electrolytes and electrodes^{5,6,16,18}. Also, most polymers used were synthetic, which are widely known for their very slow degradation rate and resultantly leads to an unintended environmental waste footprint^{21,22}. It is also worth noting that the synthetic polymers used as the base constituent for the majority of reported gel-electrolyte preparation methods are known to induce crystallinity, thus affecting the flexibility of the complete cell. These overall limitations propelled our research to look at and explore better alternatives.

This study focuses on preparing and characterizing a novel chitosan-based polymer gel electrolyte with various additives. Chitosan, a derivative of chitin, is chosen among various polysaccharides due to its ease of preparation, natural abundance, cost-effectiveness, environmentally benign nature, and its high degree of functionality that is not available in most synthetic polymers²⁵. Chitosan, previously was used in a wide variety of applications such as for controlled drug release

in pharmaceutical medical industry, exchange membranes for fuel cells, proton membranes and electrode binders in supercapacitors, binder and polymer electrolyte in Li-based batteries and in biosensors ²⁵⁻³⁵, but has never been incorporated into gel-electrolyte preparation for secondary battery applications. The ionic conductivity of pristine chitosan was approximately 10^{-6} S/cm, which is at least two orders of magnitude higher than the conventionally used synthetic polymers (PEO, PVP, etc.), predictably due to its amorphous nature. The self-gelatinous make-up of this biopolymer also facilitated film preparation ²⁵. Hence, our motif was to develop a chitosan-based polymer electrolyte to form a stable, flexible, and high ionically conducting films using PVA and KOH additives. This procedure also intends to avoid the time-consuming process of in-house polymer synthesis as a means of facility and repeatability of future works. PVA was chosen due to its ability to form thin films, ready solubility in water, good solvent retention capacity, and high temperature stability. KOH was chosen due to its fast-electrochemical kinetics and proven ability to increase ionic conductivities ^{5-7,9,12,13,18,19,23,24,28,33,36}. Conductivity measurements, as well as structural, physical, and electrochemical stability studies, were performed on the prepared chitosan-PVA-KOH electrolytes, using an optimized method from our previous studies ^{23,24}. A best average ionic conductivity of 105.04 mS/cm was obtained for our chitosan electrolyte films with 150-220 μm thickness using PVA and KOH additives.

2. EXPERIMENTAL

2.1 Preparation and incorporation of Chitosan based gel polymer electrolyte

A stage-wise preparation technique similar to our previously published ^{23,24} is adapted for electrolyte preparation. During the first stage, all polymers used were made solution processable. Chitosan (M_w -1526.4g/mol, Fischer scientific) obtained in powder form was made solution

processable by dissolving an appropriate amount (300mg) in 10 ml of 1.5% acetic acid (Sigma Aldrich) solution on a magnetic stirring assisted hot plate at 70°C and 220 rpm overnight. During the same stage, PVA (Mowiol, M_w -130,000, Sigma Aldrich) polymer crystals (600mg) were dissolved in 10 ml deionized (DI) water and magnetically stirred at 200 rpm on a hot plate at 75°C overnight. In the second stage, varying amounts of PVA (0.2, 0.4, 0.6, 0.8 and 1) were added to the chitosan solution to obtain CPx mixtures, where x indicates the amount of PVA added to obtain 1:x wt. ratio of chitosan: PVA mixture. The obtained samples are mixed using a vortex mixer for a few minutes to create a homogeneous solution. The various obtained samples were then drop-casted into silicon molds (2cm dia.) for ease of extraction. The molds with the mixture were then placed in an oven for drying at 37°C for 20 hours. The schematic shown in Figure 1 summarizes the electrolyte preparation process. Dried gel electrolytes were then removed, soaked in the 2M KOH solution and then measured.

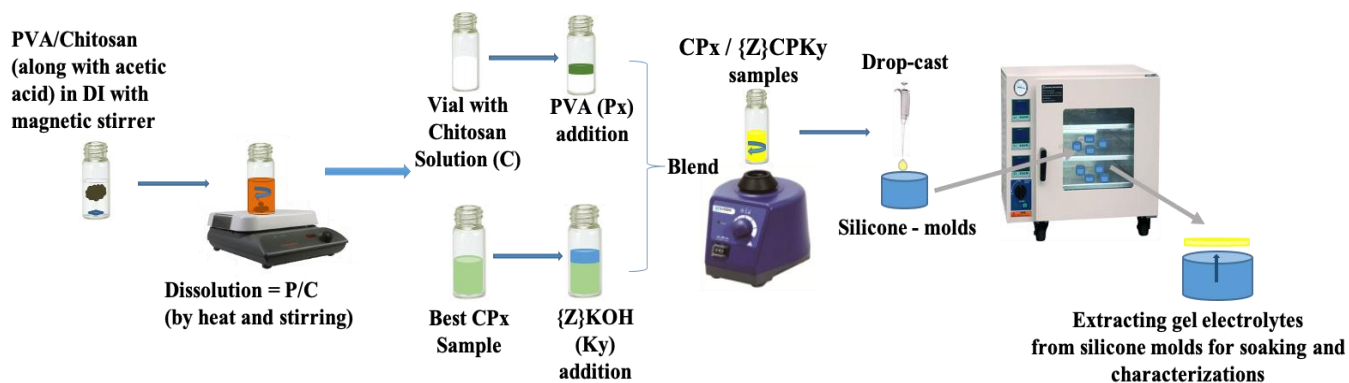


FIGURE 1. Schematic of stages involved in electrolyte preparation.

In the third stage, the best performing electrolyte CP0.2 (Chitosan: PVA=1:0.2) was chosen based on its ionic conductivity values and stability. To this CP0.2 electrolyte, varying amounts of 2M KOH (Sigma Aldrich) (0.1, 0.2, 0.3, 0.4 and 0.5) was added to form CPKy solutions individually (where CPKy= CP0.2: y [amount of 2M KOH added => 0.1-0.5]). The obtained new mixtures

were mixed, drop-casted, and dried in the same way as stage two. These obtained films were initially weighed (W1) and then soaked in a 2M KOH solution for intervals of 15 minutes until 1 hour and hereafter for intervals of 60 minutes until 3 hours. The final weights (W2) of each of the samples at each of the defined intervals were also measured. The resulting swollen films were then tested for ionic conductivities. The best performing electrolyte was found to be CPK0.3 (CP0.2: KOH=1:0.3) due to its superior ionic conductivity value. Conductivity measurements, as well as structural, physical, and electrochemical stability studies, were performed on the prepared Chitosan-PVA-KOH electrolyte samples ^{23,24}. Furthermore, a Zn-MnO₂ battery incorporating the best performing electrolyte was prepared by subsequently layering nickel foil (Fischer Scientific), Zinc foil (rolled, 99.95%, 30µm, Goodfellow), prepared polymer electrolyte, and a MnO₂ cathode ink coated Ni foil. MnO₂ cathode ink was prepared using commercial MnO₂, super-p carbon (Sigma Aldrich) and the solution processed chitosan (stage 1) in 70:20:10 ratio and sonicated for 45 minutes. All layers were then clamped in a swagelok cell for 30 minutes prior to electrochemical testing.

2.2 Characterizations and measurements

Ionic conductivities of samples at room temperature were investigated through AC electrochemical impedance spectroscopy (EIS) studies using a Versastat (Princeton applied research) from 1MHz to 100 mHz at an amplitude of 10 mV. Four samples of each of the compositions of electrolytes (CPx, CPKy) were made and measured to minimize error. The set-up used was created in-house and is similar to that of a Swagelok cell assembly, with electrolyte sandwiched between custom-built stainless steel (SS) blocking electrodes with a geometric surface of $\sim 2.5 \text{ cm}^2$. Prior to any impedance measurements, the thickness of the samples were measured using a Vernier caliper (Mityutoyo), and were calculated as the difference of measured lengths of blocking electrodes with

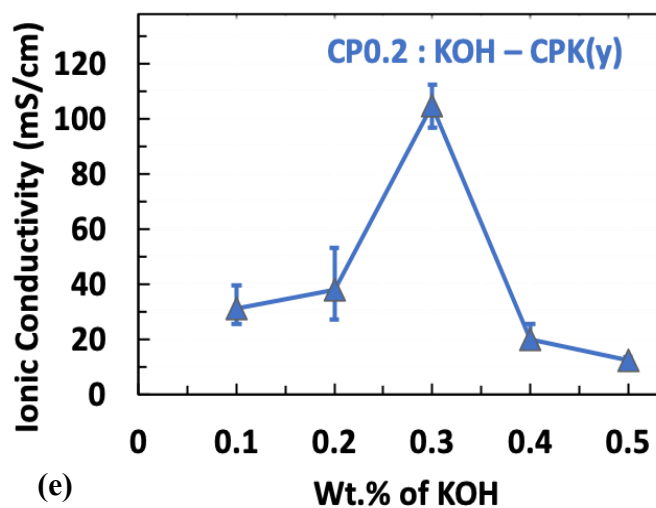
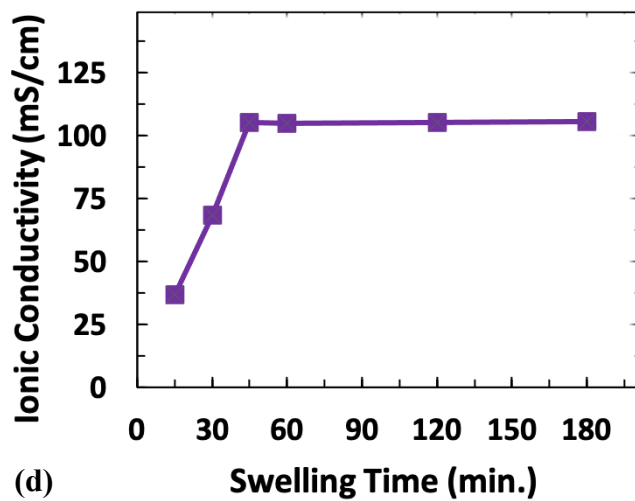
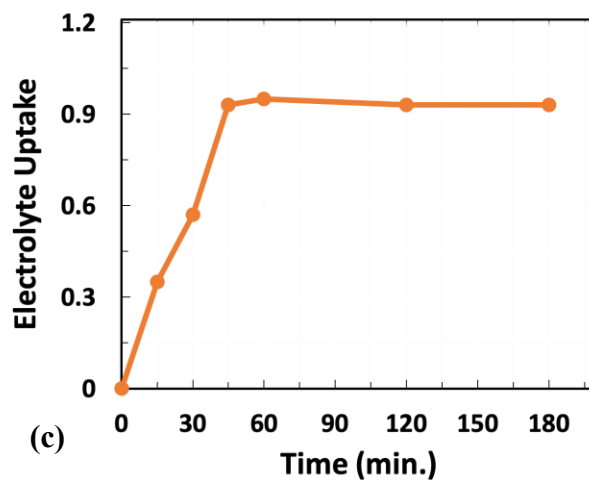
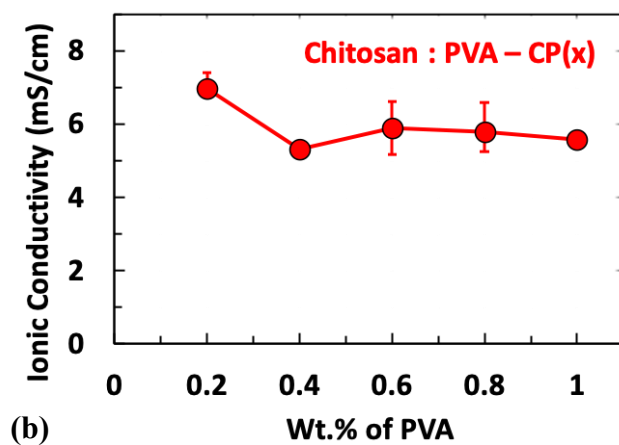
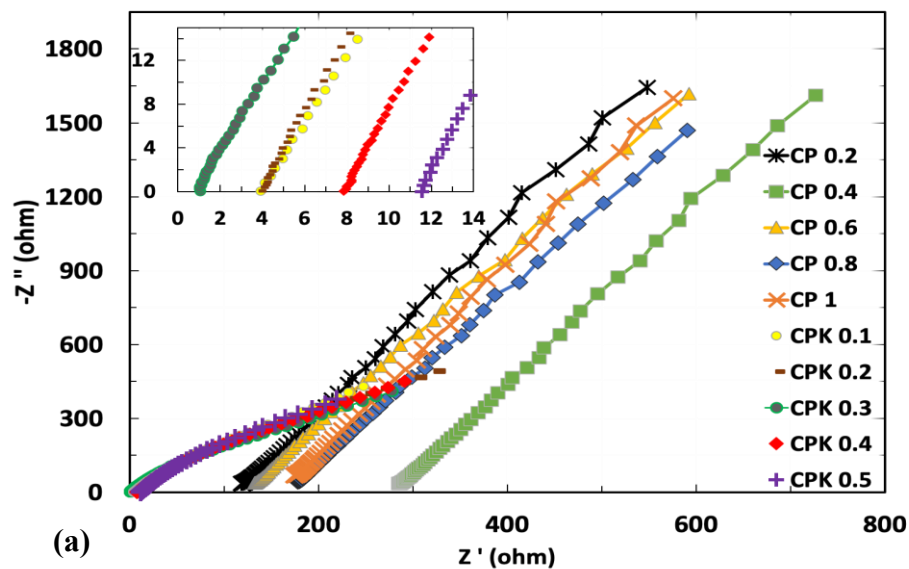
and without the electrolyte between them. These measurements were also later confirmed using a micrometer (Mityutoyo) to minimize any possible error. Optical microscopic imaging was performed using a beam reflecting and transmitting microscope (BX53M, Olympus) coupled with stream basic software for data processing of varied scans. SEM images were taken on a Nova NanoSEM 450 (FEI). XRD analysis (Rigaku mini flex) was performed using a Cu K α radiation source operating at 0.02 degree per step, 15mA and 30kV. The Fourier transform infrared (FT-IR) absorption spectra of various gel electrolytes were measured using a Frontier Optica spectroscope from Pelkin Elmer with a resolution of 2cm⁻¹, 400-4000 cm⁻¹ measuring wave number and 64 scans. Thermogravimetric analysis (TGA) of samples was conducted using a Perkin Elmer Pyris 1 thermogravimetric analyzer. The temperature range used for testing was 25-800°C with the temperature increasing at the rate of 10°C/min with He flow within the furnace. Samples suitable for mechanical testing (1.0 \pm 0.10 mm width) were fabricated from the as-prepared bulk using a razor cutting system. The specific dimensions of each sample were evaluated using optical microscopy to determine the active cross-sectional area. To enable tensile loading the as cut samples were affixed to a card stock loading frame and evaluated in a purpose-built custom loading system (details discussed later). The samples were tested in monotonic displacement control to final separation at a quasistatic strain rate of 10⁻³ 1/s using an purpose-built load frame. Measure of load was made in line with a commercially available load cell of capacity 2.45N and measure of strain was done in the sample gage section using a noncontact laser-based strain/displacement gage. Linear scan voltammetry (LSV) with potential range 0-4V at 5 mV/s and cyclic voltammetry at 10 mV/s for range 0-2V were conducted using the Versastat. Charge-discharge testing of a Zn-MnO₂ alkaline battery was performed using a battery cycler (MTI corp.).

3. RESULTS AND DISCUSSION

3.1 Impedance studies

The room temperature ionic conductivities of all samples with varying ratios of additives were obtained through AC impedance measurements extracted from Nyquist plots. A blocking electrode system, SS/Chitosan-based electrolyte/SS was used for the studies. Since blocking electrodes were used, we expect the spectra to be at an angle less than 90° due to the imperfections in alignment at the electrode-electrolyte interface. From the obtained spectra, a Nyquist plot, the bulk resistance (R_b) of samples can be extracted as the intercept of the real axis at higher frequencies. Using this R_b along with the thickness (t) of the samples, ionic conductivity is calculated using the equation $\sigma_i = t/(A * R_b)$; where A is the area of the blocking electrodes. The σ_i of pristine chitosan was calculated to be 10^{-6} S/cm, using the mentioned relation. Prior to impedance measurements, the thickness of each of the samples was measured using the method mentioned and were found to be in the range of 150-220 μ m. These values were relatively consistent for various samples of the same compositions. The samples were then placed in the in-house setup and connected to the Versastat. Figure 2a shows the impedance spectra of CPx (Chitosan-PVA) and CPKy (CP0.2-KOH samples using 2M KOH for preparation and soaking). From their analysis, 118.82-287.58 Ω and 1.06-11.64 Ω were the ranges of R_b for CPx and CPKy samples respectively. Using the relation and obtained values collectively, the ionic conductivities of each of the samples were calculated for at least 4 of each of the samples.

Interestingly, it was observed that the ionic conductivities of all CPx (Chitosan: PVA) samples increased by three orders in comparison to the pristine, irrespective of the amount of PVA added (as seen in Figure 2b). This is due to the high absorption/retention of water by PVA from the



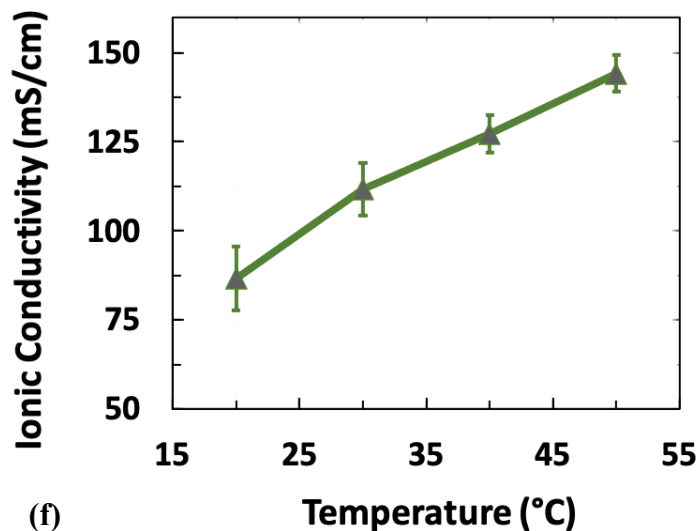


FIGURE 2. (a) AC impedance spectra of CPx (Chitosan: PVA) and CPKy (CP0.2: KOH) samples; (b) Variation in ionic conductivities of CPx samples with varied amounts of PVA; (c) Swelling ratio variation of CPK0.3 samples with time; (d) Ionic conductivity variation of CPK0.3 samples with different swelling durations; (e) Ionic conductivity trend for the samples with varying amounts of added KOH followed by soaking in 2M KOH solution for 60 minutes; (f) Variation in ionic conductivity of CPK0.3 samples with temperature.

solutions used in solvent processing stage, even after drying³⁷. All samples (CP0.2, CP0.4, CP0.6, CP0.8, and CP1) had relatively similar values when compared with each other. Though they were similar, a slight reduction in values was observed with increasing amount of PVA. This might be because of the increasing viscosity/crystallinity of the gel polymer system with increasing concentrations of PVA, causing a reduction in mobility of charge carriers³⁷⁻³⁹. This phenomenon will be discussed in detail later in structural studies (XRD analysis). The highest ionic conductivity recorded for the Chitosan-PVA system is 6.95 mS/cm for CP0.2 (chitosan: PVA=1:0.2) sample. This sample was chosen for further experimentation due to its relatively high ionic conductivity value with similar flexibility, and stability as the other films. Since only a small amount of PVA

was added to chitosan, it did not add rigidity to the gel films.

Now in efforts to further improve the ionic conductivity values varying amounts of KOH were added to CP0.2 samples to form CPK_y samples ($y = 0.1, 0.2, 0.3, 0.4$ and 0.5), which are further soaked in 2M KOH solutions for varied intervals of time. The swelling ratio (SR) for each of the samples were calculated using the relation: $SR = (W_2 - W_1)/W_1$, where W_1 indicates initial weight and W_2 final weight at a certain interval of time pre- and post-soaking, as discussed in experimental section. Swelling studies results indicated an increase in the uptake of the 2M KOH solution with increased soaking time interval. However past 60 minutes of soaking, data suggests that additional time did not benefit the electrolyte uptake. Figure 2c shows the highest SR value of 0.95 recorded for the CPK0.3 sample along with the SR variation trend with time. As can be observed from figure 2d, ionic conductivities measured at corresponding intervals also indicated a similar trend as the swelling uptake. A highest ionic conductivity of 105.04 mS/cm was observed for the CPK0.3 sample soaked for 45 minutes. We assume this improvement in ionic conductivity to be result of improved uptake of the 2M KOH electrolytic solution, resulting in more ions readily able to transport³⁷⁻³⁹. Soaking beyond 45 minutes did not help in improving the ionic conductivity of the sample, similar to the trend that has been observed in the swelling experiment. Thus, 60 minutes of soaking time was deduced optimal post data analysis and was further used for all additional CPK_y electrolytes preparation for conductivity measurements.

Figure 2d shows the best ionic conductivities of the prepared and 60 minutes soaked various CPK_y samples. When observing the effect of adding varied amounts of 2M KOH, it was observed that the ionic conductivities increased with increasing salt content until 30 wt. % (1:0.3 ratio). This

increase in conductivity values may be due to the increase in the number of mobile ions in the polymer gel, which are generated due to the dissociation of the added KOH salt ³⁹. Also, within this salt content range (i.e., 30 wt. %), it is safe to say that the rate of ion dissociation is greater than the rate of ion association, due to the increased conductivity values. As previously noted, sample CPK0.3 recorded the highest ionic conductivity value of 105.04 mS/cm when compared within the CPKy system. Beyond this 30 wt. % (0.3 ratio) of 2M KOH salt addition, the ionic conductivity values decreased. It may be due to the short distance between the dissociated ions resulting from higher concentrations of salt giving them the ability to recombine and form neutral ion pairs that do not contribute towards ionic conductivity ³⁹. Also, another probable cause might be the increase in the viscosity of the solution during the third stage of electrolyte preparation with increasing salt content, also seen in the case of PVA addition, which leads to appearance of crystalline phase in polymer membrane system. The latter leads to a chemistry with inflexible polymer chains, and thus greatly reducing the migration ability of OH⁻ ions in the membrane ^{39,40}. As can be observed from Table 1, the highest ionic conductivity, i.e. 105 mS/cm obtained for the CPK0.3 sample, is comparable to most polymer electrolyte systems reported thus far.

Additionally, ionic conductivities of CPK0.3 sample at various temperatures were also measured. As can be seen in Figure 2f, a linear relationship between the ionic conductivity and operating temperature was observed, i.e., with an increase in temperature, there is a subsequent increase in ionic conductivity. To mention one, the soaked CPK0.3 sample at room temperature (20°C, measured during winter) recorded ~63% of the ionic conductivity of the identical one maintained at 50°C. We assume this improved conductivity is a result of better ion transport facilitation due to thermal movement of polymer chains and dissociation of salts from the electrolytic solution

with increased temperatures. This phenomenon of improved ion transport with temperature is in agreement with previous polymer electrolyte-based studies ¹¹⁻¹³. This relation is especially beneficial for our study, as most secondary cells operate at temperatures above that of room temperature when in continuous operation and thereby possibly result in enhanced performances than reported.

Polymer electrolyte composition	σ_i (mS/cm)	Ref. #	Polymer electrolyte composition	σ_i (mS/cm)	Ref. #
PEO-KOH	1	6-15	PVA-KOH-H ₂ O	1	13
PVA-KOH	0.85	9	GGPE (gelatin-based polymer gel electrolyte)	3.1	11
PVA-PEO-glass fiber mat-KOH	10	5	PVA-Chitosan-NH ₄ Br	0.768	28
PVDF-PC-EC-ZnTf	3.94	16	Chitosan acetate-NH ₄ CH ₃ COO-EC	3.83	29
PAN-PC-EC-ZnTf	2.67	17	Plasticized chitosan-PEO-NH ₄ NO ₃ -EC	2.06	32
PVA-PAA-KOH	300	12	PVA-Plasticized chitosan- NH ₄ NO ₃	1.6	32-38
PVA-KOH-PEGDE	220	18	PVA-Bamboo charcoal-KOH	66.3	40
PEG-PVA-(NH ₄ CH ₂ CO ₂) ₂	3.7	7	Chitosan-adipic acid	~ 4	34
PVA-KOH hydrogel	340	19	Chitosan-acetic acid	~ 2.5	
Gelatin-PAM	26.5	20	NFC hydrogel-gelatin-KOH	90	23
Gelatin-PAM-PAN	17.6		NFC hydrogel-PVA-KOH	75	24
Chitosan-PVA-KOH	105	Present work			

TABLE 1. Ionic conductivity values of various polymer electrolyte compositions used in varied applications.

3.2 Structural Studies

Microscopic imaging and FT-IR analysis were performed on the pristine and best samples (CP0.2 and CPK0.3) at each stage of electrolyte preparation to better understand how conductivity improved in relation to morphological and structural bond changes occurring in the films. Also,

XRD analysis was performed on the different PVA added samples (CPx) to better understand the ionic conductivity changes.

Figures 3a-c show the reflected beam micrographs of pristine chitosan, 20 wt. % PVA added chitosan (CP0.2), and 30 wt.% 2M KOH added CP0.2 sample (CPK0.3) respectively. The micrograph of the pure chitosan film (Figure 3a) indicates the surface of the film to be smooth and homogeneous with the exception of evenly wide-spread tiny crystalline structures found throughout the sample. This may be the major reason for the low ionic conductivity values of pristine chitosan films ⁴¹. Figure 3b, the micrograph of CP0.2 (best CPx sample) also depicts a uniform surface throughout the film but with additional PVA chains. For obtaining the micrograph of this particular sample, an extended focal length image collection through process managing was conducted. This was performed because the sample was visibly translucent compared to the pristine sample. The obtained concatenated image shows and confirms the presence of chitosan crystals, PVA chains, and the solution trapped in between. The amorphous nature of the gel electrolyte, due to the incorporation of PVA, thus explains the increase in conductivity values ^{15,16,23,36}.

With the addition of 30 wt. % KOH to CP0.2, the surface of the gel sample (CPK0.3) shares similarities to that of a sponge in appearance, i.e., pores distributed on the surface of the membranes with KOH in between and can be seen in Figure 3c. To confirm said pores, a higher magnification micrograph was also collected and is inserted in Figure 3c. The transmitting beam micrograph (Figure 3d) of the CPK0.3 sample shows an illuminated region, where light passes through the polymer network, indicating the film to be porous inside as well and confirming the

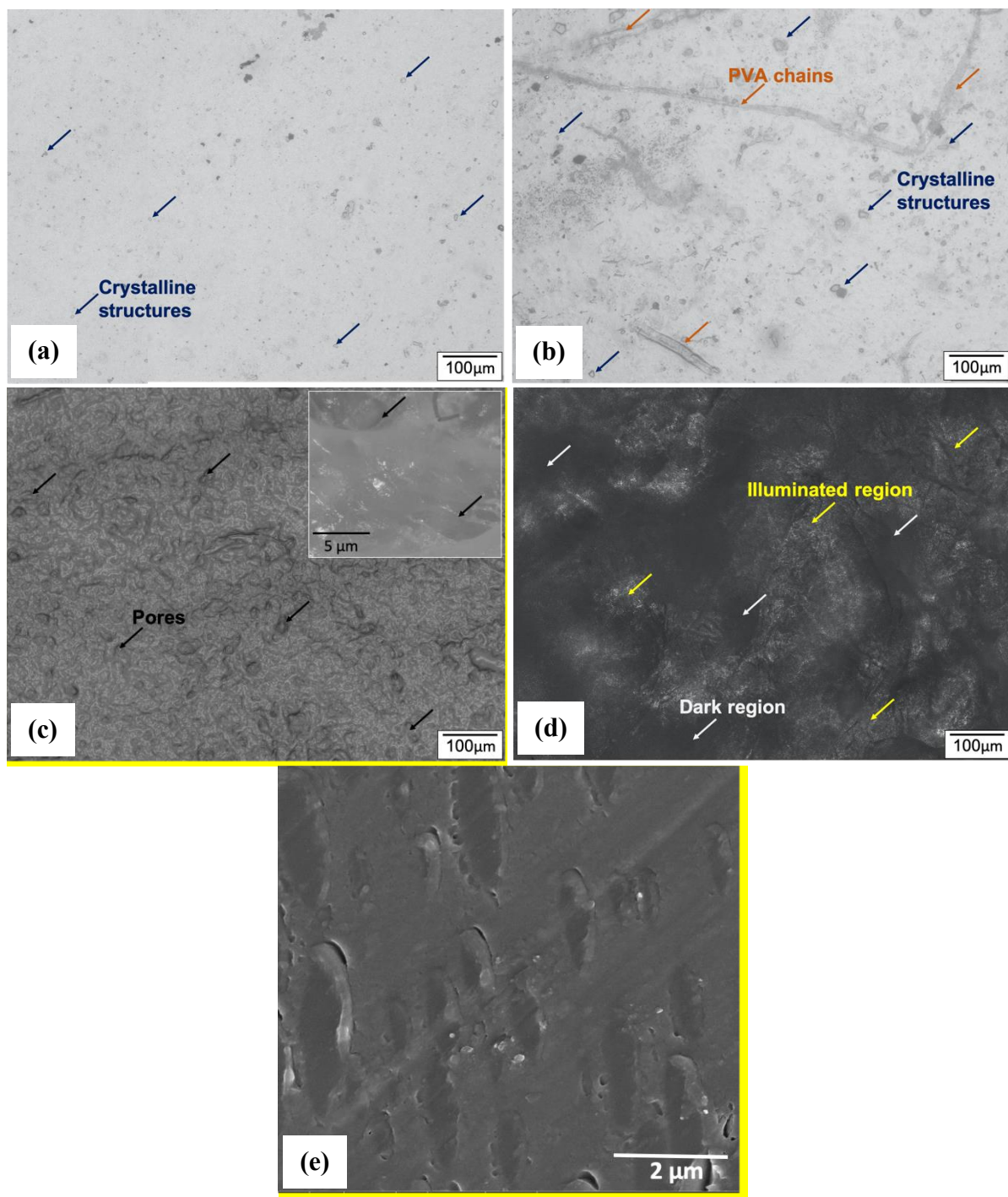


FIGURE 3. Reflected beam optical micrographs of (a) Pristine Chitosan, (b) Chitosan with 20 wt.% PVA (CP0.2), and (c) CP0.2 with 30 wt.% 2MKOH (CPK0.3) respectively; (d) Transmitting beam optical micrograph of CPK0.3; and (e) Scanning electron micrograph of CPK0.3 sample.

formation of 3D network. This formation allows for more KOH to be retained within the polymer framework, thus providing more ions readily available for chemical reactions and as a result increases the conductivity of the films ^{39,41}. Figure 3d also shows dark regions, which we hypothesize is a result of the loss of light due to multiple reflections over the polymer framework along the path. SEM micrograph was also obtained for CPK0.3 sample to verify previous claims of sample composition. As can be observed from figure 3e, the sample does in fact exhibit a pore-like matrix suitable for the absorption and retention of liquid electrolytes. This patterned pore matrix, as previously detailed, directly attributes to the increase in ionic conductivity of the electrolyte with PVA and KOH additives.

Figure 4a shows the FT-IR spectra of pristine chitosan, CP0.2, and CPK0.3. This study was performed to confirm the restructuring of bonds due to the addition of additives to pure chitosan. Spectral analysis was performed on each of the solutions, i.e., the solution-processed chitosan, CP0.2 solution, and CPK0.3 solution from their respective stages in electrolyte preparation. Analysis of the chitosan spectra shows peaks around 3421 to 3300 cm^{-1} that represents a strong O-H bond and its axial stretch due to the presence of an alcohol group ^{42,43}. The peak around 2926 cm^{-1} indicates medium C-H stretch in alkanes, and the peak at 1687 cm^{-1} indicates medium N-H stretch bend due to the amine group of chitosan ⁴². Peaks around 1442 cm^{-1} and 1480 cm^{-1} indicate the C-H stretching of CH_2 and CH_3 groups. The small, tiny peaks around 1296 cm^{-1} are due to the strong C-N stretch present in amines. Single peaks at 1158 cm^{-1} , 1061 cm^{-1} and the simultaneous four peaks between 912 cm^{-1} and 1023 cm^{-1} are due to strong C-O-C stretching. Similarly, analysis of pure PVA and KOH were also performed. PVA spectra exhibited peaks at 3438 cm^{-1} , 2923 cm^{-1} , 1726 cm^{-1} , and 1656 cm^{-1} . The broad peak at 3438 cm^{-1} and the subtle peak around 2923 cm^{-1}

indicate stretching of hydroxyl groups due to C-H stretching. The peak observed at 1726cm^{-1} corresponds to C=O, and that around 1656cm^{-1} corresponds to stretching of C=C hydroxyl groups. The latter were in agreement with previous studies^{23,24}. KOH spectra causes stretched O-H bond with a broad peak at $\sim 3410\text{cm}^{-1}$ and also agrees with earlier studies^{23,24}. Addition of 20 wt. % PVA (0.2 ratio) to chitosan resulted in relaxing of most stretches observed in pristine polymers, thus confirming definite changes in bonds. Further, the addition of 30 wt. % KOH (0.3 ratio) to CP0.2 indicated re-emergence of few characteristic peaks between 1023cm^{-1} and 1158cm^{-1} . Also, small disturbances in between the characteristic peaks indicating vibrations⁴¹⁻⁴³ in bonds were observed. Overall, the FT-IR spectra results are indicative of changes in all the samples pertaining to the effect of different additives.

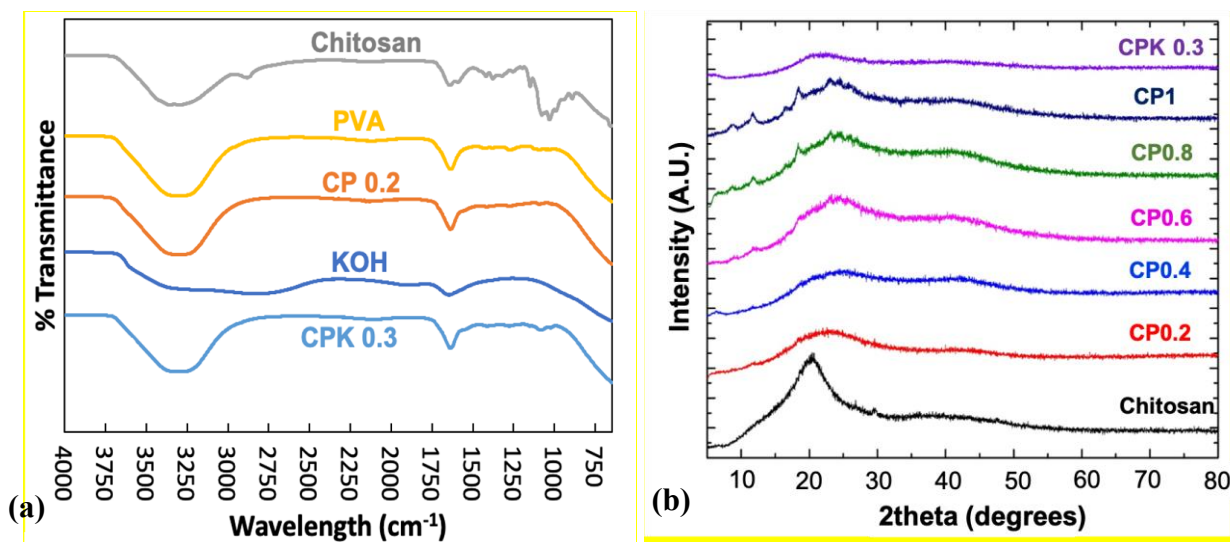


FIGURE 4. (a) FT-IR spectra of pure Chitosan, PVA, KOH, CP0.2 and CPK0.3 samples.; (b) XRD spectra of pure chitosan, CPx (0.2-1), and CPK0.3

The results of XRD analysis for pure chitosan, the CPx system, and CPK0.3 are shown in figure 4b. As previously described, the addition of PVA to pure chitosan is known to increase the amorphous behavior of the films¹². A similar conclusion can be made by comparing the XRD patterns of chitosan pre- and post- PVA addition (CPx), as well as after the incorporation of KOH

(CPK0.3). At $2\theta = 20^\circ$, a broad diffraction peak with high intensity is observed from the pure chitosan sample, indicating a higher degree of crystallinity. It is characteristic of pure chitosan to display diffraction peaks, indicating diffractions from (020) and (110) planes of the chitosan crystalline lattice²⁵. With addition of different amounts of PVA, it can be observed that the characteristic peak broadness increases, and intensity decreases as a result of cross-linking of PVA with chitosan. This confirms the increase in the amorphous nature of the gel matrix with the addition of PVA. However, an insurgence of tiny peaks signifying an increase in crystallinity was observed with increasing amount of PVA when comparing CPx samples only. This explains the slight reduction in ionic conductivity values resulting from reduced mobility of charge carriers for higher amounts of PVA added samples^{12, 28}, as observed earlier in conductivity studies. Furthermore, with addition of KOH to the CP0.2 sample, CPK0.3, we observe a heightened amorphous domain of the film as evident by the relaxation of all peaks and thus validates the improved conductivity values^{23,24}.

3.3 Stability Studies

3.3.1 Physical

Various stability tests were performed on the prepared electrolytes. The strength, flexibility, and stability of the best-prepared gel electrolyte, i.e., CPK0.3, was tested through a manual cyclic bending test. The latter flexure test is conducted by taking hold of the sample at two points and loading the midpoint of the circular film repeatedly, alternating directions. There were no recovery periods between flexure cycling. Figures 5a-c show the sample before, during, and after testing respectively. The sample was manually bent as shown in Figure 5b for 250 cycles continuously. No cracks or ruptures of the sample were observed after completion of the test. This indicated that the sample was strong and flexible. However, after complete bending cycles, slight plastic

deformation of the sample was observed as can be seen in Figure 5c. This permanent curving of the sample may lead to a bad contact between the layers in the battery and may cause degradation of performance in long run if they need to be incorporated in battery applications that need to undergo continuous major bending and recovery. An average ionic conductivity of 95.4 mS/cm was recorded from impedance testing of CPK0.3 samples post-250 cycles bending. The post cycling value is 90.9% that of the averaged CPK0.3 value (105.05 mS/cm) which had not undergone cyclic bending. Having only about a 10% decrease in ionic transport efficiency, the post-cycle sample is able to retain most of its performance capability despite having undergone plastic deformation. We assume the decrease in ionic conductivity post-bending is probably due to the loss of electrolyte's embedded electrolytic solution when bending continuously in ambient conditions. The latter suggests that this electrolyte has the potential to perform in flexible secondary battery applications given that it remains fully assembled between electrodes and enclosed.

The mechanical properties of the chitosan electrolyte systems were also studied in order to develop a more thorough understanding of its potential in flexible full cell application. As can be observed from figure 5d, the razor cut samples are frame mounted and then affixed to the mechanical loading train. Once affixed into the load train the sample carrier frame edges are cut, resulting in a free-standing chitosan/CP0.2/CPK0.3 sheet for testing in direct tension. A noncontact laser strain/displacement measure method enabling the direct measurement of sample strain/displacement was used. The laser strain/displacement gage eliminates parasitic effects of rigid body motion in the samples and possible reinforcement from adhered strain measurement methods. The results obtained from testing are presented as tensile stress-strain curves (as seen in

Figure 5e), with pure chitosan used as a control. The deformation nature of the control can be described as typical of a ductile polymer,

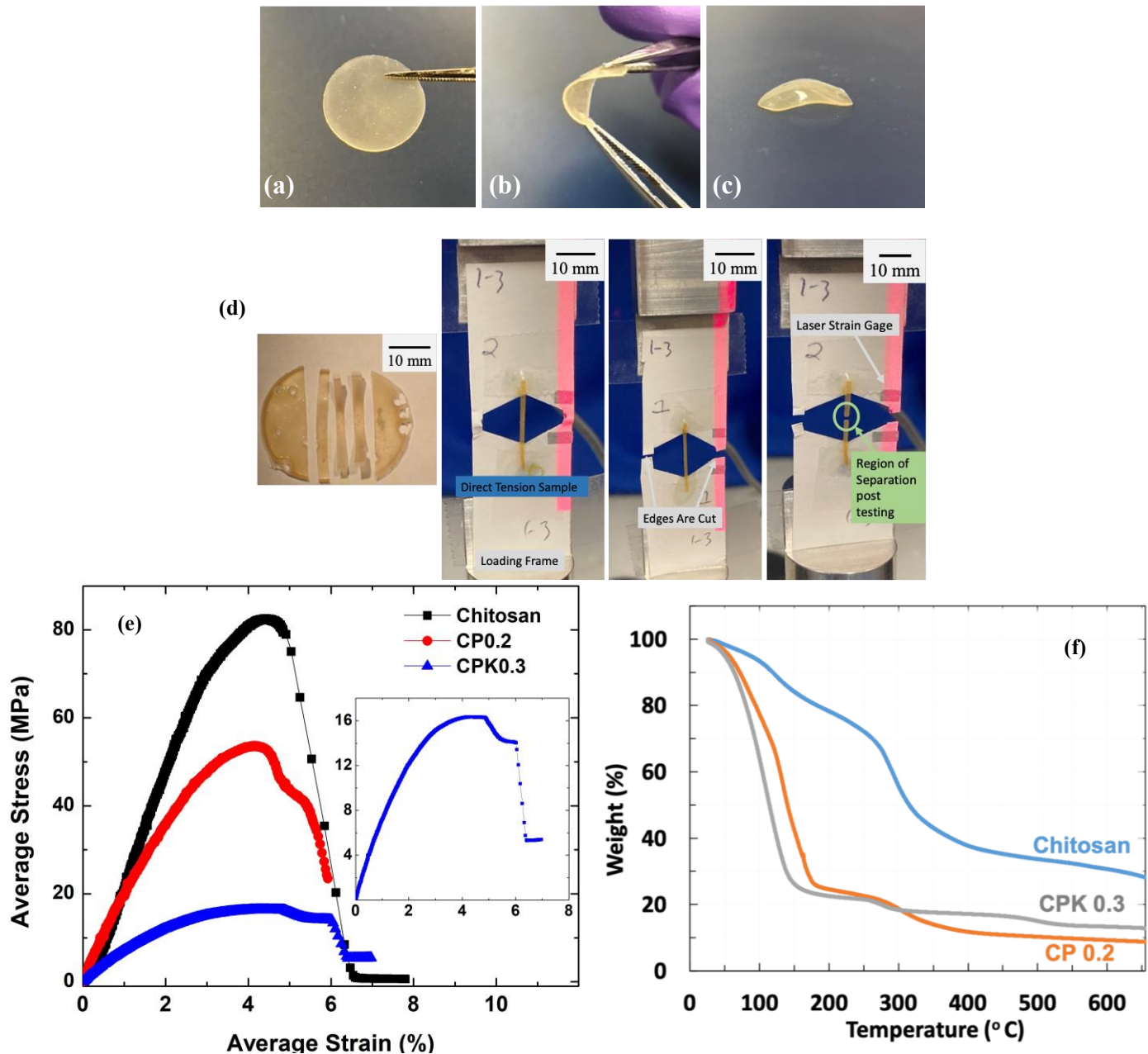


FIGURE 5. Images of CPK0.3 sample (a) before, (b) during, and (c) after 250 cycles manual bending test respectively; (d) Images of a sample razor cut to desired dimensions and its tensile testing procedure showing the sample, loading and post mortem; (e) Monotonic Tensile stress-

strain curves of Chitosan, CP0.2 and CPK0.3 samples; (f) Thermograms of Chitosan, CP0.2 and CPK0.3 samples.

as it exhibits both a steep elastic region at low strains, indicative of its elastic moduli, and a plateau of stress at higher strains, reflective of its ductile properties ⁴⁴. This stress-strain behavior is somewhat similar for CPK0.3, however not representative of CP0.2. In CP0.2 a muted elastic region is observed, however the lack thereof plateaued region indicates a significant loss in ductility of the sample. This observation may lend itself to the heightened crystallinity within the CP0.2 sample, as its curve represents a more rigid and brittle polymer material. The inset in figure 5e distinctively displays CPK0.3 in order to better note its two characteristic regions. The heightened ductile nature of CPK0.3 is likely due to the amorphous inner pore matrix of the membrane, resulting from the incorporation of KOH. And although the incorporation of additives to the control may reduce its excellent stress properties, for the intended application of this material, and in comparison, to other reported values, it can be said that sample CPK0.3 is a suitable candidate ⁴⁴⁻⁴⁸. Table 2 displays the measured mechanical properties of the chitosan electrolyte systems explored in this study.

	C	CP0.2	CPK0.3
Young's Modulus (MPa)	2712.6	1837.9	700.33
Yield Strength (MPa)	43.136	30.519	7.1998
UTS (MPa)	82.59	53.639	16.333
Strain to Failure (%)	4.91	5.5	6.02

TABLE 2. Mechanical properties of pure Chitosan, CP0.2, and CPK0.3 samples.

Thermal stability studies of pristine chitosan, CP0.2, and CPK0.3 films were conducted using TGA analysis and the obtained thermograms are shown in Figure 5f. It can be seen that chitosan

undergoes a two-stage degradation. The first stage weight loss of about 20% was observed between 50 °C and 150°C and is attributed by the moisture vaporization from polar groups of chitosan molecules ^{49, 50}. Subsequently, a drastic weight loss of about 40% was observed during the second stage degradation of chitosan between 275 and 380°C. This was due to the thermal degradation of chitosan chains ^{40-43, 49-50}. Later on, slight weight loss continued until 650°C due to the burning out of the degraded backbone ^{49, 50}. Similarly, CP0.2 and CPK0.3 also observed a two-stage degradation. A drastic weight loss of about 74% and 76% were observed respectively for CP0.2 and CPK0.3 samples between 50 and 175°C. This was mainly due to the vaporization of solvents and alkaline solution retained by films due to the addition of PVA and KOH. Beyond that, slight degradations of about 3% and 5% were observed for CP0.2 and CPK0.3 respectively. This was attributed collectively to the cleavage of the backbone of chitosan and PVA matrix between 310 and 350°C ^{41-43, 49}. Thus, the analysis confirms that the polymer electrolyte CPK0.3 prepared is completely safe to be used in room temperature operating batteries and is also stable until 50°C.

3.3.2 Electrochemical

The best sample CPK0.3 was also tested using a linear scan voltammetry experiment (LSV). It was performed to determine the potential range for its electrochemical stability. To perform LSV, the electrolyte was placed between zinc electrodes. The anodic stability of the electrolyte was determined by applying a sweeping voltage until 4V at a scan rate of 5mV/s followed by monitoring of the resulting current density values. Figure 6a shows the resultant voltammogram. Analysis of the voltammogram indicates that the sample CPK0.3 showed negligible current densities between 0 and 2V, with respect to the zinc electrode. Beyond which, an increase in currents is observed, indicating changes occurring within the electrolyte. Thus, the prepared

CPK0.3 gel electrolyte can provide the necessary electrochemical stability for a battery operating under 2V.

Cyclic voltammetry of CPK0.3 sample against zinc electrodes, scanned at 10 mV/s with a voltage window of 0-2.0 V is shown in Figure 6b. From the curve obtained, we can observe occurrence of both oxidation and reduction peaks at 1.575 V and 0.349 V, respectively, suggesting the successful ion mobility within the assembled cell. The potential difference (ΔE_p) was calculated to be 1.226 V. A corresponding anodic peak current (i_a) of 0.346 mA, and a cathodic peak current (i_c) of 0.38013 mA were obtained as can be observed from the figure. Overall, the voltammetry tests conducted indicate the electrolyte to be electrochemically stable and to be suitable for further electrochemical testing in full cell construction.

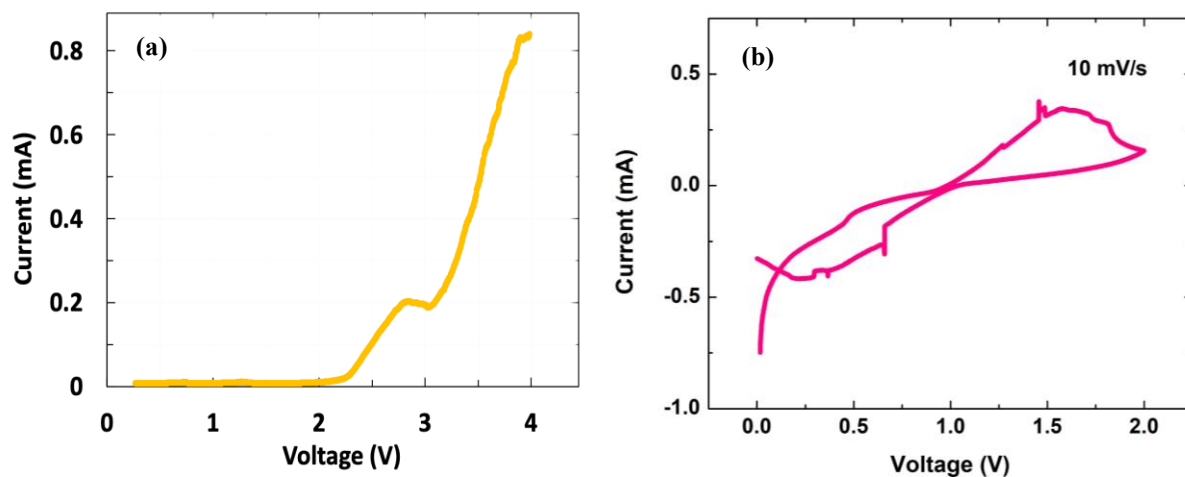


FIGURE 6. (a) Linear scan voltammogram for CPK0.3 sample at sweep rate of 5mV/s; (b) Cyclic voltammogram of a Zn/CPK0.3/Zn cell swept at 10 mV/s.

3.4 Cell testing

Figure 7 details the cycling capability of the prepared Zn/CPK0.3/MnO₂ cell tested within a voltage range of 0.2 - 1.8 V. A galvanostatic charge-discharge test was conducted for 20 cycles at

0.5A/g. The charge/discharge profiles obtained for the first five cycles can be seen in Figure 7a. It was observed that for all five cycles the voltage of the battery drops immediately before reaching a flat discharge plateau of ~ 1.1 - 1.2 V, indicating presence of concentration polarizations at electrode surfaces within the constructed cell and possible zinc passivation^{51, 52}. The highest specific capacity of 221.6 mAh/g was achieved for the assembled battery with novel highly ionically conducting biodegradable polymer electrolyte. However, a significant capacity fade of $\sim 75\%$ w.r.t. initial cycle was observed within the first five cycles. We assume this sharp capacity drop is likely due to a combination of Zn passivation and δ -MnO₂ formation, resulting in reduced active material availability for further electrochemical reactions. Beyond five cycles, the battery performance was observed to be relatively stable with 97% coulombic efficiency for 20 cycles. Though the obtained performance is not ideal in terms of material utilization and needs to be further improved for practical feasibility, it is similar to that of aqueous Zn-MnO₂ alkaline batteries with no additives⁵³. Overall, the results indicate successful preparation and incorporation of the highly ionically conducting novel chitosan-based alkaline electrolyte in a Zn-MnO₂ system in addition to accommodating redox reactions responsible for the working of the battery. We believe the findings presented in this work will allow the use of a flexible, eco-friendly, highly ionically conducting alkaline electrolyte in a Zn-MnO₂ instead of a traditional aqueous alkaline electrolyte causing overall battery packaging and flexibility hindrances.

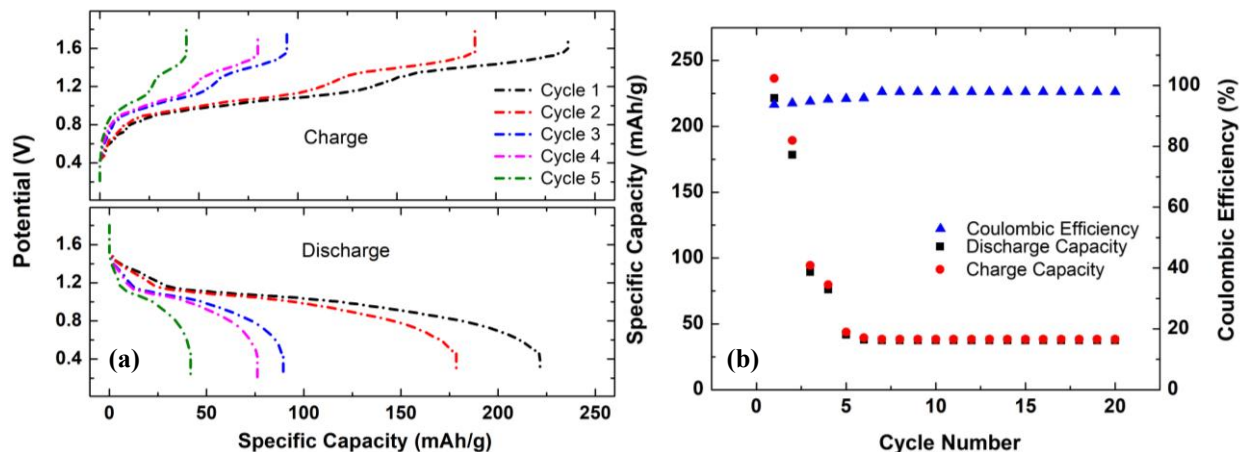


Figure 7. (a) Galvanostatic charge/discharge profiles of Zn/CPK0.3/MnO₂ cell at 0.5 A/g between 0.2 and 1.8V; (b) Cycling performance and corresponding coulombic efficiency at 0.5 A/g.

4. CONCLUSION

We present a scalable, energy, and time efficient preparation method for developing high ionically conductive chitosan-based PVA-KOH polymer gel electrolytes, with a best sample (CPK0.3) ionic conductivity of 105.04 mS/cm. The results for conductivity obtained by these novel gel electrolytes are comparable with not only other reported solid-state gel electrolytes, but also with conventional liquid or aqueous electrolytes reported. Extensive morphology and structural studies were conducted on these electrolytes to reinforce the mechanical, electrochemical, and thermal efficiency of the films. In addition to achieving films with high ionic conductivity, the aforementioned studies suggest high flexibility, strength, temperature stability, and cycle life for our electrolyte films. Additionally, the prepared electrolytes are compatible for zinc-based chemistries and are electrochemically stable under 2V potential.

ACKNOWLEDGEMENTS

The authors would like to thank the University of Maryland, Baltimore County (UMBC) for

supporting this research from startup fund. The authors would also like to thank Eunhwa Jang, Preetham Gowni and Renmar Sarreal for their contributions.

REFERENCES

1. Dunn, B.; Kamath, H.; Tarascon, J. M., *Science* 334, 928 2011.
2. Larcher, D.; Tarascon, J. M., *Nat Chem* 7, 19 2015.
3. Li, H. F.; Ma, L. T.; Han, C. P.; Wang, Z. F.; Liu, Z. X.; Tang, Z. J.; Zhi, C. Y., *Nano Energy* 62, 550 2019.
4. Zhang, S. S., *J Power Sources* 164, 351 2007.
5. Yang, C. C.; Lin, S. J., *J Power Sources* 112, 497 2002.
6. Guinot, S.; Salmon, E.; Penneau, J. F.; Fauvarque, J. F., *Electrochim Acta* 43, 1163 1998.
7. Patel, S. K.; Awadhia, A.; Agrawal, S. L., *Phase Transit* 82, 421 2009.
8. Tsuchida, E.; Ohno, H.; Tsunemi, K., *Electrochim Acta* 28, 591 1983.
9. Mohamad, A. A.; Mohamed, N. S.; Yahya, M. Z. A.; Othman, R.; Ramesh, S.; Alias, Y.; Arof, A. K., *Solid State Ionics* 156, 171 2003.
10. Tsunemi, K.; Ohno, H.; Tsuchida, E., *Electrochim Acta* 28, 833 1983.
11. Park, J.; Park, M.; Nam, G.; Lee, J. S.; Cho, J., *Adv Mater* 27, 1396 2015.
12. Wu, G. M.; Lin, S. J.; Yang, C. C., *J Membrane Sci* 280, 802 2006.
13. Lewandowski, A.; Skorupska, K.; Malinska, J., *Solid State Ionics* 133, 265 2000.
14. Hagan, W. P.; Latham, R. J.; Linford, R. G.; Vickers, S. L., *Solid State Ionics* 70, 666 1994.
15. Fauvarque, J. F.; Guinot, S.; Bouzir, N.; Salmon, E.; Penneau, J. F., *Electrochim Acta* 40, 2449 1995.
16. Kumar, G. G.; Sampath, S., *Solid State Ionics* 160, 289 2003.

17. Kumar, G. G.; Sampath, S., J Electrochem Soc 150, A608 2003.
18. Merle, G.; Hosseiny, S. S.; Wessling, M.; Nijmeijer, K., J Membrane Sci 409, 191 2012.
19. Santos, F.; Tafur, J. P.; Abad, J.; Romero, A. J. F., J Electroanal Chem 8502019.
20. Li, H. F.; Han, C. P.; Huang, Y.; Huang, Y.; Zhu, M. S.; Pei, Z. X.; Xue, Q.; Wang, Z. F.; Liu, Z. X.; Tang, Z. J.; Wang, Y. K.; Kang, F. Y.; Li, B. H.; Zhi, C. Y., Energ Environ Sci 11, 941 2018.
21. Barbalata, D. F. A., Synthetic Polymers: Technology, properties, applications; Journal of the American Chemical Society: Chapman & Hall: Florence, 1997.
22. Molyneux, P.; CRC Press, Taylor & Francis Group, Boca Raton: 2018.
23. Poosapati, A.; Jang, E.; Madan, D.; Jang, N.; Hu, L. B.; Lan, Y. C., Mrs Commun 9, 122 2019.
24. Poosapati, A.; Negrete, K.; Jang, N.; Hu, L. B.; Lan, Y. C.; Madan, D., Mrs Commun 9, 1015 2019.
25. Rinaudo, M., Prog Polym Sci 31, 603 2006.
26. Chai, L. L.; Qu, Q. T.; Zhang, L. F.; Shen, M.; Zhang, L.; Zheng, H. H., Electrochim Acta 105, 378 2013.
27. Subban, R. H. Y.; Arof, A. K.; Radhakrishna, S., Mat Sci Eng B-Solid 38, 156 1996.
28. Yusof, Y. M.; Illias, H. A.; Kadir, M. F. Z., Ionics 20, 1235 2014.
29. Alias, S. S.; Chee, S. M.; Mohamad, A. A., Arab J Chem 10, S3687 2017.
30. Aziz, S. B.; Abdullah, O. G.; Rasheed, M. A.; Ahmed, H. M., Polymers-Basel 9,2017.
31. Smitha, B.; Sridhar, S.; Khan, A. A., Macromolecules 37, 2233 2004.
32. Shukur, M. F.; Ithnin, R.; Illias, H. A.; Kadir, M. F. Z., Opt Mater 35, 1834 2013.
33. Kadir, M. F. Z.; Arof, A. K., Mater Res Innov 15, 217 2011.

34. Chupp, J.; Shellikeri, A.; Palui, G.; Chatterjee, J., *J Appl Polym Sci* 132, 2015.
35. Yamagata, M.; Soeda, K.; Ikebe, S.; Yamazaki, S.; Ishikawa, M., *Electrochim Acta* 100, 275 2013.
36. Bhad, S.; V.S.Sangawar, *Chemical Science Transactions* 1, 653 2012.
37. Wang, Z. Q.; Winslow, R.; Madan, D.; Wright, P. K.; Evans, J. W.; Keif, M.; Rong, X. Y., *J Power Sources* 268, 246 2014.
38. Ho, C. C.; Evans, J. W.; Wright, P. K., *J Micromech Microeng* 20,2010.
39. Kadir, M. F. Z.; Majid, S. R.; Arof, A. K., *Electrochim Acta* 55, 1475 2010.
40. Fan, L. D.; Wang, M. Y.; Zhang, Z.; Qin, G.; Hu, X. Y.; Chen, Q., *Materials* 112018.
41. M.Z.A, Y.; Harun, K.; Ali, A. M. M.; M.F, M.; M.A.K.M, H.; Ibrahim, S.; Mustaffa, M.; Z.M, D.; Abdul latif, F., *Journal of Applied Sciences* 62006.
42. Mulchandani, N.; Shah, N.; Mehta, T., *Polym Polym Compos* 25, 241 2017.
43. Navaratnam, S.; Ramesh, K.; Ramesh, S.; Sanusi, A.; Basirun, W. J.; Arof, A. K., *Electrochim Acta* 175, 68 2015.
44. Wan, Y., Creber, K. A. M., Peppley, B., Bui, V. T. J. *Memb. Sci.*, 2006, 284, 331–338.
45. Han, J., Huang, Y., Chen, Y., Song, A., Deng, X., Liu, B., Li, X., Wang, M. *ChemElectroChem*, 2020, 7, 1213–1224.
46. Kim, S. H., Choi, J. K., Bae, Y. C. *J. Appl. Polym. Sci.*, 2001, 81, 948–956.
47. Wang, M., Fan, L., Qin, G., Hu, X., Wang, Y., Wang, C., Yang, J., Chen, Q. *J. Memb. Sci.*, 2020, 597, 117740.
48. Clark, R., Averbach, B. In *OCEANS '78* 1978; 82–86.
49. Tripathi, S.; Mehrotra, G. K.; Dutta, P. K., *Int J Biol Macromol* 45, 372 2009.
50. Bajpai, M.; Bajpai, S. K.; Jyotishi, P., *Int J Biol Macromol* 84, 1 2016.

51. Biswal, A., Tripathy, B. C., Sanjay, K., Subbaiah, T., Minakshi, M. RSC Adv., 2015, 5, 58255–58283
52. Powers, R. W., Breiter, M. W. J. Electrochem. Soc., 1969, 116, 719.
53. Liu, X., Yi, J., Wu, K., Jiang, Y., Liu, Y., Zhao, B., Li, W., Zhang, J. Nanotechnology, 2020, 31, 122001.